Minimum Transfer Times for Nonperfectly Reflecting Solar Sailcraft

Bernd Dachwald*
DLR, German Aerospace Center, 51147 Cologne, Germany

Introduction

SOLAR sailcraft trajectory analyses are typically made for high-performance sailcraft under the assumption that the solar sail is either an ideal reflector or by consideration of the nonideal reflectivity through an overall efficiency factor that reduces the magnitude of the solar radiation pressure (SRP) force but leaves its direction unaltered.[1−3] In both cases, the SRP force model is a model of perfect, that is, specular, reflection because the direction of the SRP force is always perpendicular to the sail surface. For a thorough mission analysis, however, one must consider the optical properties of the real nonperfectly reflecting sail film, where the SRP force also has a component parallel to the sail surface. Taking the current state-of-the-art in engineering of ultralightweight structures into account, solar sailcraft of the first generation will be of relatively moderate performance. The simplification of perfect reflectivity and the limitation on high-performance sailcraft seem both to be caused mainly by the difficulty of generation of an adequate initial guess for traditional local trajectory optimization methods. As a smart method for global trajectory optimization, artificial neural networks can be combined with evolutionary algorithms to form so-called evolutionary neurocontrollers (ENCs).[4] Evolutionary neurocontrol (ENC) does not require an initial guess. By the use of ENC, near globally optimal trajectories can also be calculated for nonperfectly reflecting solar sailcraft of moderate performance.

In the sequel, after the different SRP force models have been defined, minimal transfer times for rendezvous missions within the inner solar system will be presented for perfectly and nonperfectly reflecting solar sailcraft, including a near-Earth asteroid rendezvous ($1996FG_3$) and a main belt asteroid rendezvous (Vesta).

SRP Force Models

Different levels of simplification for the characteristics of a solar sail result in different models for the magnitude and direction of the SRP force acting on the sail. The most simple model assumes an ideally reflecting sail surface. It will here be denoted as model ideal reflection (IR). It can be easily derived[5] that the force exerted on an ideally reflecting solar sail is

$$\boldsymbol{F}_{\mathrm{SRP}}(r,\beta) = 2P(r)A\cos^2\beta\,\boldsymbol{n} \tag{1}$$

where $P(r) = P_0 \cdot (1\mathrm{AU}/r)^2$ is the SRP. [$P_0 = 4.563\ \mu\mathrm{N/m}^2$ is the SRP at 1 astronomical unit (AU) and r is the distance from the sun.] A is the sail area, $\boldsymbol{n}$ is a unit vector that is perpendicular to the sail surface and always directed away from the sun (sail normal vector), and β is the angle between the sun line and $\boldsymbol{n}$ (sail cone angle). It will become convenient to also introduce a thrust unit vector $\boldsymbol{f}$ that is always along the direction of the SRP force. For model IR, $\boldsymbol{f} = \boldsymbol{n}$.

With the intention to model the nonideal reflectivity of a solar sail, an overall sail efficiency factor η is typically used in the solar sail related literature that reduces only the magnitude of the SRP force, but leaves its direction unaltered. This model will be denoted as model η-perfect reflection (ηPR). The SRP force acting on the sail is in this case

$$\boldsymbol{F}_{\mathrm{SRP}}(r,\beta,\eta) = 2\eta P(r)A\cos^2\beta\,\boldsymbol{n} \tag{2}$$

so that, again, $\boldsymbol{f} = \boldsymbol{n}$.

For a thorough trajectory simulation, a more sophisticated SRP force model must be employed that takes into account the optical parameters $\boldsymbol{p}$ of the real sail film. This model will be denoted as model nonperfect reflection (NPR). It was proposed in the 1970s for solar sailcraft trajectory optimization by Sauer,[6] and it was further studied by Forward[7] but found little application since then except in a paper by Cichan and Melton.[8] Using model NPR, it can be shown[5,9] that the SRP force acting on the sail has a component

$$F_\perp = 2P(r)Aq_\perp(\beta,\boldsymbol{p}) \tag{3}$$

perpendicular to the sail surface and a component

$$F_\parallel = 2P(r)Aq_\parallel(\beta,\boldsymbol{p}) \tag{4}$$

parallel to the sail surface. For a sail with a highly reflective aluminum-coated front side and a highly emissive chromium-coated back side (to keep the sail temperature within moderate limits), using the optical parameters given by Wright,[9] one gets

$$q_\perp(\beta,\boldsymbol{p}_{\mathrm{Al|Cr}}) = 0.9136\cos^2\beta - 0.005444\cos\beta \tag{5}$$

$$q_\parallel(\beta,\boldsymbol{p}_{\mathrm{Al|Cr}}) = 0.0864\sin\beta\cos\beta \tag{6}$$

The SRP force acting on the sail may be written as

$$\boldsymbol{F}_{\mathrm{SRP}} = \sqrt{F_\perp^2 + F_\parallel^2}\,\boldsymbol{f} \tag{7}$$

and likewise by defining

$$Q^2(\beta,\boldsymbol{p}) = \sqrt{q_\perp^2(\beta,\boldsymbol{p}) + q_\parallel^2(\beta,\boldsymbol{p})} \tag{8}$$

as

$$\boldsymbol{F}_{\mathrm{SRP}}(r,\beta,\boldsymbol{p}) = 2P(r)AQ^2(\beta,\boldsymbol{p})\boldsymbol{f} \tag{9}$$

For model NPR, $\boldsymbol{f} \neq \boldsymbol{n}$; the angle between $\boldsymbol{n}$ and $\boldsymbol{f}$ is $\varepsilon = \arctan(q_\parallel/q_\perp)$.

All three SRP force models do not take into account the shape of the sail film under load, but assume a plane sail surface. Recently, Colasurdo and Casalino[10] presented a model that is a simplified (no diffuse reflection and equal emissivity on both sail sides) version of model NPR. Their model, which should not be confused with model ηPR (because they choose the symbol η for the reflectivity, not for the overall sail efficiency), will not be considered in the reminder of this Note.

The models IR and ηPR, where $\boldsymbol{f} = \boldsymbol{n}$, allow an easy analytical treatment of solar sail steering problems. If $\boldsymbol{d}$ denotes the unit vector along the desired thrust direction, the thrust unit vector $\boldsymbol{f}$ must point into the direction $\boldsymbol{f}^*$ that maximizes the SRP force along $\boldsymbol{d}$; $\boldsymbol{f}^*$ can be derived analytically from $\boldsymbol{d}$, which is given by the optimizer, that is, by the neurocontroller. The problem is to determine the sail normal vector that maximizes the SRP force along the desired thrust direction $\boldsymbol{n}^*$, so that $\boldsymbol{f} = \boldsymbol{f}^*$. For models IR and ηPR, $\boldsymbol{n}^* = \boldsymbol{f}^*$. For model NPR, $\boldsymbol{n}^*$ cannot be calculated analytically from $\boldsymbol{f}^*$ because the $Q^2(\beta,\boldsymbol{p})$ expression cannot be resolved for β. Although the models IR and ηPR allow the analytical treatment of solar sail steering problems, they misrepresent $F_\perp$ and completely ignore $F_\parallel$. In doing so, both models ignore the deviation of $\boldsymbol{f}$ from $\boldsymbol{n}$. This deviation becomes larger as β increases, that is, as the sail moves closer edge-on to the incoming radiation. As a consequence, the SRP force in model NPR is not only smaller than in model IR (which is also taken into account by model ηPR), but is also much more constrained in its direction.

Figure 1 shows for each SRP force model the "bubble" on whose surface the SRP force vector tip is constrained to lie (vector tail

Received 5 November 2003; revision received 13 February 2004; accepted for publication 12 March 2004.

*Research Engineer, Institute of Space Simulation. Member AIAA.

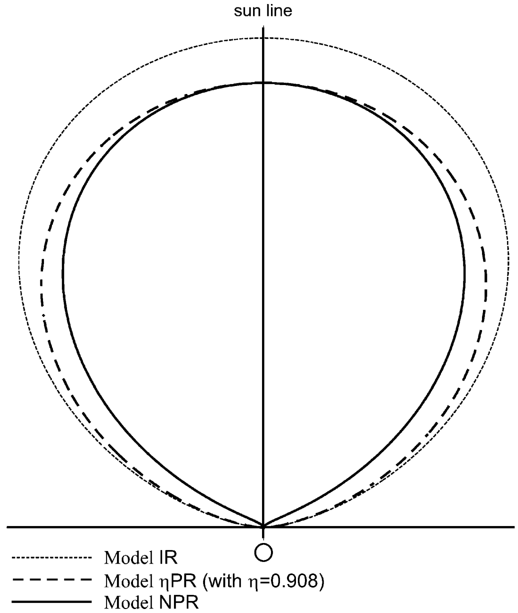

Fig. 1 SRP force bubbles.

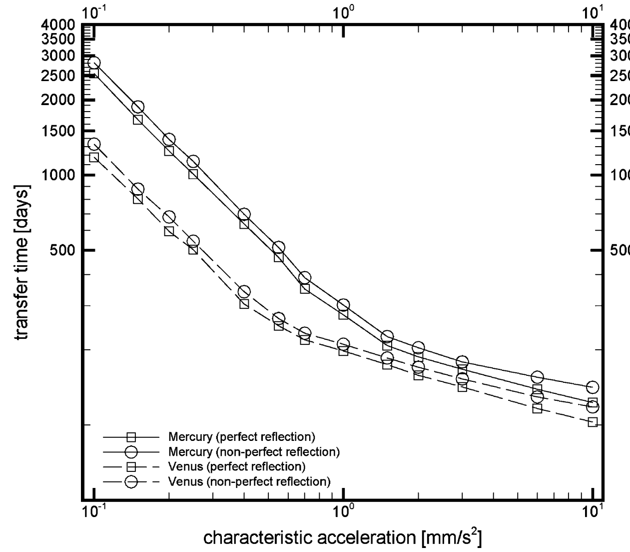

Fig. 2 Minimal orbit transfer times for Mercury and Venus.

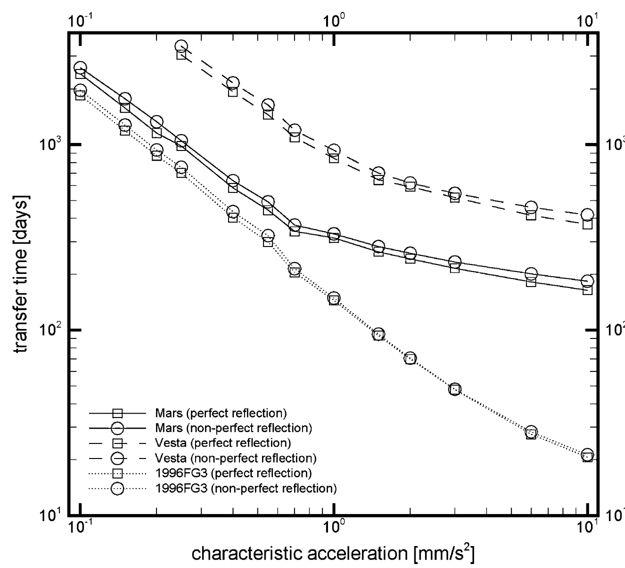

Fig. 3 Minimal orbit transfer times for Mars, Vesta, and 1996FG$_3$.

at origin). From the perspective of trajectory analysis, model ηPR is equivalent to model IR because the shape of both bubbles is identical. A decrease in sail efficiency η can always be offset with a proportional increase in sail area, so that both bubbles have the same shape and size. There is no similar equivalence for model NPR. Even if the $\cos^2\beta$-bubble and the $Q^2(\beta, \boldsymbol{p})$-bubble are scaled to the same size, their shape is different.

The prevalent performance parameter for solar sailcraft is the characteristic acceleration a_c, defined as the SRP acceleration acting on a solar sail that is oriented perpendicular to the sun line at 1AU. For model ηPR, one gets $a_c = 2\eta P_0 A/m$. For model NPR one gets $a_c = 2q_\perp(0, \boldsymbol{p}) P_0 A/m$. To get the same a_c for model ηPR and model NPR, one has to set $\eta = q_\perp(0, \boldsymbol{p})$, which is about 0.908 for an Al|Cr-coated sail.

Simulation Model

Ideally, all forces acting on the sailcraft have to be considered for a thorough mission analysis. However, for mission feasibility analysis, as done here, only preliminary trajectory analysis needs to be done, which allows for some simplifications: 1) The solar sailcraft is moving under the sole influence of solar gravitation and radiation, where the sun is a point mass and a point light source. 2) The solar sailcraft's attitude can be changed instantaneously. 3) The sail film does not degrade over time.

By the use of ENC for global trajectory optimization and the trajectory optimization software GESOP with SNOPT for fine tuning the ENC trajectories, the minimal transfer times to various solar system bodies have been calculated for characteristic accelerations in the range $0.1\ \text{mm/s}^2 \le a_c \le 10.0\ \text{mm/s}^2$, with model ηPR and model NPR. For all calculations, the size of the SRP force bubbles was the same ($a_{c,\text{NPR}} = a_{c,\eta\text{PR}}$). To obtain the globally (or at least near globally) optimal orbit transfer times, the true longitude at launch was left free, and the final boundary constraints were set to $\Delta r \le 10^6$ km and $\Delta v \le 0.5$ km/s, where Δr and Δv is the final distance and relative velocity, respectively, of the sailcraft to a virtual body that is on the target orbit and has the same true longitude. Note that the solution of this orbit transfer problem yields the absolute minimum transfer time, independent of the constellation of the initial and the target body. The optimal launch constellation for the rendezvous problem can then be deduced from the optimal solution of the orbit transfer problem.

Numerical Results

For perfectly reflecting high-performance sailcraft, with $0.5\ \text{mm/s}^2 \lesssim a_c \lesssim 2.5\ \text{mm/s}^2$, the ENC results presented in Fig. 2 and 3 are consistent with the results obtained by Sauer[1] for minimal transfer times to Mercury, Venus, and Mars. Additionally, the ENC results presented here reveal two performance regimes: moderate-performance sailcraft ($a_c \lesssim 0.5\ \text{mm/s}^2$) and high-performance sailcraft ($a_c \gtrsim 1.0\ \text{mm/s}^2$). Within both regimes, the minimum transfer times $T_{\min}$ can be approximated with very simple functions of the form

$$\tilde{T}_{\min} = c_1 \big/ \tilde{a}_c^{c_2} \tag{10}$$

where $\tilde{T}_{\min} = T_{\min}/1$ day and $\tilde{a}_c = a_c/1\ \text{mm/s}^2$. Besides the performance regime, the values for c_1 and c_2 obviously depend on the target body. It can be speculated that they are a function of the initial and the target body's orbital elements. For example, the approximation function

$$\tilde{T}_{\min,\text{Mercury}} = 280/\tilde{a}_c$$

gives for $0.1\ \text{mm/s}^2 \le a_c \le 0.55\ \text{mm/s}^2$ and model NPR a maximum error of 1.55% for the Earth–Mercury transfer. Within the high-performance regime, the flight time gain due to a better sail performance is smaller. Between the two regimes, the curves bend sharply. Because the optimal trajectories for solar sailcraft to spiral inward (maximize $-\dot{a}$) or outward (maximize $+\dot{a}$) are logarithmic spirals, the reduced flight-time gain in the high-performance regime is more pronounced for the near-circular planetary target orbits, which require an additional velocity increment for a final circularization of the spiral (so that $\boldsymbol{v}_{\text{sailcraft}} \uparrow\uparrow \boldsymbol{v}_{\text{target}}$). For the transfer to the highly eccentric asteroid 1996FG$_3$ ($e = 0.35$), where such a circularization is not required, the curve bends at higher characteristic accelerations, and the bending is less pronounced.

The results also show that there is a considerable increase of up to 15% in minimal orbit transfer time if model NPR is used. The mean increase is about 10% for Mercury, Venus, Mars, and Vesta and about 5% for 1996FG$_3$. The results are in accordance with results obtained by Cichan and Melton,[8] where, using a local trajectory optimization method (direct collocation method), an increase of 7.8% in transfer time had been obtained for a simple Earth–Mars transfer ($a_c \doteq 1.5$ mm/s^2, ENC yields 6.8% for this transfer). For a simple Earth–Venus transfer, an increase of even 24% in transfer time (306 days for $a_c \doteq 0.55$ mm/s^2) had been obtained by Cichan and Melton, which suggests, however, that the trajectory is far from the global optimum (ENC yields a minimum transfer time of 267 days for exactly the same problem). The results are also in good accordance with the results obtained by Colasurdo and Casalino[10] for optimal transfers between coplanar circular orbits.

Conclusions

Minimal transfer times for rendezvous missions to inner solar system bodies have been calculated for perfectly and nonperfectly reflecting solar sailcraft, extending, thereby, the currently available data to moderate-performance sailcraft and to very-high-performance sailcraft. Two performance regimes have been found, one for moderate-performance sailcraft and one for high-performance sailcraft, in which the minimum transfer times can be approximated with very simple functions. For nonperfectly reflective solar sailcraft there is a considerable increase of about 10% in the minimal transfer times as compared to perfectly reflective solar sailcraft. The results demonstrate that, for a thorough mission analysis, the nonperfect reflectivity of the solar sail must be considered through an appropriate SRP force model. The simplification that the nonideal reflectivity of the sail can be taken into account by the use of an overall efficiency factor η should only be made for very preliminary mission feasibility analyses.

References

[1] Sauer, C. G., "Optimum Solar-Sail Interplanetary Trajectories," AIAA Paper 76-792, Aug. 1976.

[2] Leipold, M., Seboldt, W., Lingner, S., Borg, E., Herrmann, A., Pabsch, A., Wagner, O., and Brückner, J., "Mercury Sun-Synchronous Polar Orbiter with a Solar Sail," *Acta Astronautica*, Vol. 39, No. 1, 1996, pp. 143–151.

[3] Leipold, M., Pfeiffer, E., Groepper, P., Eiden, M., Seboldt, W., Herbeck, L., and Unkenbold, W., "Solar Sail Technology for Advanced Space Science Missions," International Astronautical Federation, IAF Paper 01-S.6.10, Oct. 2001.

[4] Dachwald, B., "Optimization of Interplanetary Solar Sailcraft Trajectories Using Evolutionary Neurocontrol," *Journal of Guidance, Control, and Dynamics*, Vol. 27, No. 1, 2004, pp. 66–72.

[5] McInnes, C. R., *Solar Sailing. Technology Dynamics and Mission Applications*, Springer-Verlag, London, 1999, pp. 38–40 and 47–51.

[6] Sauer, C. G., "A Comparison of Solar Sail and Ion Drive Trajectories for a Halley's Comet Rendezvous Mission," AIAA Paper 77-104, Sept. 1977.

[7] Forward, R. L., "Grey Solar Sails," *Journal of the Astronautical Sciences*, Vol. 38, No. 2, 1990, pp. 161–185.

[8] Cichan, T., and Melton, R., "Optimal Trajectories for Non-Ideal Solar Sails," American Astronautical Society, AAS Paper 01-471, Aug. 2001.

[9] Wright, J. L., *Space Sailing*, Gordon and Breach, Philadelphia, 1992, pp. 227, 228.

[10] Colasurdo, G., and Casalino, L., "Optimal Control Law for Interplanetary Trajectories with Nonideal Solar Sail," *Journal of Spacecraft and Rockets*, Vol. 40, No. 2, 2003, pp. 260–265.

D. Spencer
Associate Editor

Three-Dimensional Hypersonic Flow Computations over Reentry Capsule Using Energy Relaxation Method

M. M. Patil,* S. Swaminathan,† and R. Kalimuthu*
Vikram Sarabhai Space Center,
Thiruvananthapuram 695 022, India
and
J. C. Mandal‡
Indian Institute of Technology,
Bombay 400 076, India

Nomenclature

Cp	=	coefficient of pressure
D	=	base diameter, m
E	=	total energy, N/m^2
$\bar{\boldsymbol{F}}$	=	flux vector
M	=	Mach number
$\bar{\boldsymbol{N}}$	=	source-term vector
n	=	unit normal
p	=	pressure, N/m^2
R_N	=	nose radius, m
S	=	surface area, m^2/wave speed in Harten–Lax–van Leer contact, m/s
t	=	time, s
$\boldsymbol{U}$	=	conserved variable vector
u	=	x component of velocity, m/s
V	=	velocity, m/s
Vol	=	volume, m^3
v	=	y component of velocity, m/s
w	=	z component of velocity, m/s
α	=	angle of attack, deg
γ	=	specific heat ratio
γ_1	=	specific heat ratio corresponding to
ε	=	internal energy, m^2/s^2
ε_1	=	internal energy governed by the polytropic law, m^2/s^2
ε_2	=	internal energy advected in the flow, m^2/s^2
λ	=	relaxation rate
ρ	=	density, kg/m^3
Φ	=	internal energy function

Subscripts

i, j, k	=	cell index number along x, y, z, respectively
n	=	unit normal component
x	=	x component
y	=	y component
z	=	z component
1	=	parameters corresponding to ε_1

Superscripts

l	=	left state variable
n	=	time level

Received 13 December 2003; revision received 16 March 2004; accepted for publication 23 March 2004.

*Scientist, Kerala State.
†Division Head, Launch Vehicle Design Group, Kerala State.
‡Associate Professor, Department of Aerospace Engineering, Maharashtra State.